PHYSICAL REVIEW E **72**, 025203(R) (2005)

Effect of thermal annealing and compression on the stability of microwrinkle patterns

Takuya Ohzono[1] and Masatsugu Shimomura[1,2]
[1]*Dissipative-Hierarchy Structures Laboratory, Spatio-Temporal Function Materials Research Group, Frontier Research System, RIKEN, 2-1 Hirosawa, Wako, Saitama 351-0198, Japan*
[2]*Research Institute for Electronic Science, Hokkaido University, N21W10, Sapporo, 001-0021, Japan*
(Received 29 July 2004; published 18 August 2005)

We find that annealing followed by uniaxial compression affects the microwrinkle pattern, which originally shows a complex stripe phase, and its stability to mechanical perturbation. We observe a characteristic quasi-biaxial stripe pattern after unloading compressive stress in contrast to the case without annealing, which shows the retrieval of the original pattern. Moreover, another loading-unloading cycle in a different direction induces a change in the modulated pattern, indicating that the pattern is no longer stable to mechanical perturbations.

DOI: 10.1103/PhysRevE.72.025203 PACS number(s): 89.75.Kd, 61.41.+e, 61.25.Hq, 68.35.Gy

Microwrinkles [1–4] on a surface-modified elastomer spontaneously appear upon sample cooling due to mechanical instability such as Euler buckling [5–9]. Stripe phases are formed as widely found in nature [10–18]. Surface strain states can strongly influence this pattern [1–4]. Figure 1(a) illustrates a spontaneously formed complex stripe pattern (wavelength: ~ 1 μm) of microwrinkles after the deposition of an 8-nm-thick Pt layer over a smooth polydimethylsiloxane (PDMS) elastomer surface by ion sputtering [19]. During Pt deposition, the sample is thermally expanded. The surface is chemically modified into the silicalike rigid nature by the sputtering energy [1,2]. Then it is covered by Pt, resulting in the hardened skin layers holding the expanded state. As the temperature decreases after deposition, two-dimensionally isotropic residual compressive strain arises in the hard skin due to the difference in the thermal expansion coefficients. The surface buckles (wrinkles), showing a complex pattern with a wide distribution of stripe orientations and a characteristic wavelength [1–4].

While most studies have focused on the wrinkle formation [20–24] and the static state patterns [1–4], little is known about the pattern stability and dynamics under external mechanical or thermal perturbation. At room temperature, it has been studied that the complex pattern reversibly changes the stripe orientation depending on the external strain, and the original pattern itself is retrieved after unloading strain [19,25]. That is, the basin of attraction of the original pattern on the associated potential surface is assumed to be very large at the state without external strain. However, the mechanism of the formation of the pattern with the memory was unknown.

Our focus here is to investigate whether or not an appropriate perturbation can modulate the potential surface in the state without external strain and create different minima that correspond to different patterns from the original one. Such a perturbation, if it exists, provides knowledge of the relevant factor on the creation of the pattern memory. Technologically, if this is possible by a simple practical method, different stripe patterns on nanomicroscales with different memories can be easily realized. It would provide an interesting addition to potential technological applications of this system.

We consider an irreversible process involved in wrinkle formation. Analogous to the process of common hot-melt molding, we assume that the pattern remains fixed (frozen) at room temperature by the suppression of viscous flow, which occurs slightly in the vicinity of the surface at a high temperature (i.e., at the initial stage of wrinkling) according to the displacement of wrinkling. The spontaneous organization of wrinkles triggers the viscous flow at a high temperature, and the flow stops due to the temperature decrease at the end of pattern formation. Here, in order to demonstrate this assumption, we investigate the effect of external strain in the lateral direction during the pattern formation (wrinkling) process on the pattern and its stability against mechanical perturbation at room temperature. Simulations using a model with the memory effect are also conducted to support the assumption.

The sample of a 5-mm-thick right circular cylinder with a diameter of 8 mm is used. Pt deposition is conducted on one side with the flat surface with the circular shape. To address pattern formation repeatedly for a sample, we conduct annealing, (150 °C, 10 min, in air) followed by natural cooling at ambient conditions (20 °C). The heating relaxes the residual strain, which leads to surface flattening, and also activates the material flow initializing the memory. Exponential temperature drops are observed. The temperature reaches 20 ± 1 °C within 10 min of the cessation of heating. The pattern formation is completed within this period. During this cooling (from 150 to 20 °C) process, uniaxial compressive strain is maintained in order to perturb the pattern formation. At the beginning of the strain application (at 150 °C), the surface is flat. As the temperature drops, wrinkles evolve. The observation by an optical microscope is conducted at one specific part near the center of the circled surface to avoid edge effects and inhomogeneous strain distribution due to the circular form of the cylindrical sample.

Figure 1(b) illustrates the pattern formed under 7% compressive strain in the x direction using a vise during the cooling process. External strain is held at 20 °C for a while for observation. The result shows a simple stripe pattern in the direction parallel to the strain with some defects [12]. Subsequently, external strain is unloaded (at the rate of $-1\%/\mathrm{min}$) to obtain the pattern in the state without external strain [Fig. 1(c)] at 20 °C, where the internal residual strain

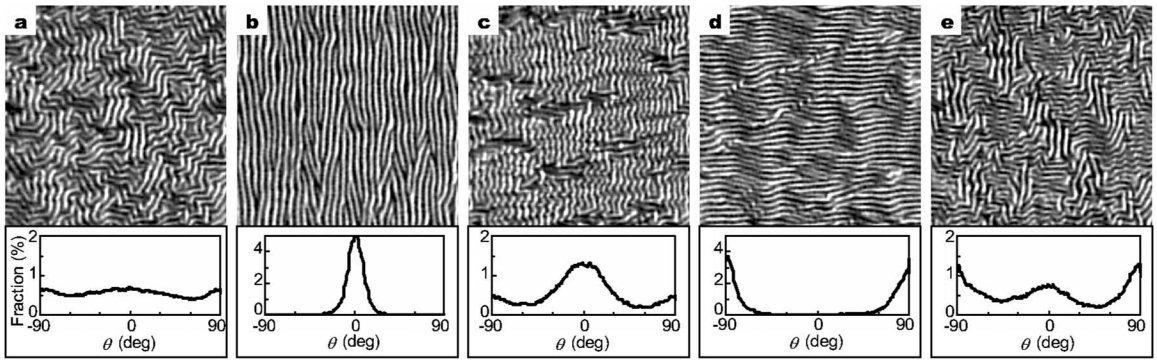

FIG. 1. Sequential pattern changes due to annealing and strain exertions by experiments. The upper panels show optical micrographs of the identical area (35×35 μm^2) on a specific sample. The lower panels show histograms of the corresponding stripe orientation θ that is calculated at each point in the image based on the method by Egolf [19,26] where θ is the angle between the wave direction and the x axis, and is defined within a range from $-90°$ to $90°$ due to the C_2 symmetry. (a) A complex stripe pattern formed without external strain. (b) The aligned stripe pattern formed under external compressive strain in x (0°) after heating. At this point, external strain is held. (c) The quasibiaxial stripe pattern formed after strain unloading. (d) and (e) Subsequently formed aligned and quasibiaxial patterns under the same ACU process as those in (b) and (c), respectively, except for the strain direction, $y(\pm90°)$.

is almost isotropic. Contrary to the pattern in Fig. 1(a), the stripe orientation exhibits a quasibiaxial distribution. The high and low peaks in the stripe orientation histogram correspond to the parallel and vertical directions in which the strain is exerted, respectively. The isotropic residual strain is relaxed by the coexistence of both domains with orientations perpendicular to each other. The domains with the vertical orientation to the exerted strain direction mainly appear from the topological defects [Figs. 1(b) and 1(c)] and show slightly different wavelengths. Hereafter, the sequential process of annealing, cooling under strain, and unloading is abbreviated as the ACU process at room temperature.

We repeat the same ACU process, changing the strain direction to y, for an identical sample. Figure 1(d) illustrates the strained state, where strain was applied at the beginning of cooling process after annealing and held. Figure 1(e) illustrates the state after strain unloading at 20 °C. It shows a qualitatively similar trend except for the stripe orientation. The repeated trend (at least 10 times) in various strain directions is observed. The quasibiaxial patterns prepared using an ACU process remain unchanged (at least for 1 week).

The direction of exerted strain during the pattern formation repeatedly controls the orientational nature of the quasibiaxial pattern. This result suggests that the memory of the original complex pattern is erased or weakened and that the system is trapped in a different minimum on the associated potential surface after the ACU process.

Figures 2(a)–2(d) show the instability of the quasibiaxial pattern at room temperature against perturbation of the successive compression (7%) and unloading (at the rate of $\pm1\%/\mathrm{min}$). Predictably, the quasibiaxial stripes [Fig. 1(e)] are aligned to the strain direction when the strain is held [Figs. 2(a) and 2(d)]. In contrast to the previous study [19], the resultant patterns in the state without external strain change into different quasibiaxial or disordered patterns depending on the strain directions [Figs. 1(c) and 1(d)]. This state lacks the robust memory that leads to the retrieval of the initial pattern. The ACU process creates many local metastable states, which correspond to the quasibiaxial or disordered patterns.

Figure 2(e) indicates that subsequent annealing and cooling without external strain results in a pattern that is almost

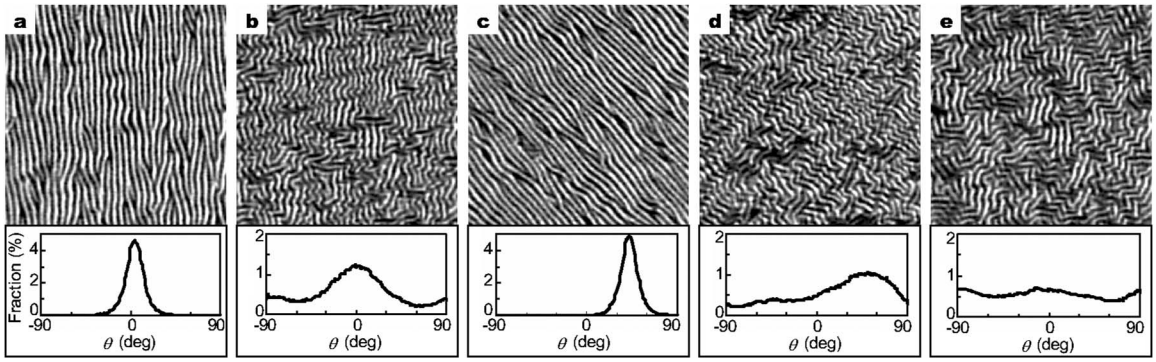

FIG. 2. Sequential pattern changes due to strain exertions continued from Fig. 1. Identical areas to those in Fig. 1 are displayed in the upper panels. The lower panels show the corresponding stripe orientation histograms. (a) The stripe pattern aligned by external compression in x (0°) without annealing from the pattern in Fig. 1(e). (b) The quasibiaxial stripe pattern formed after strain unloading. (c) and (d) Subsequently formed aligned and quasibiaxial patterns under the same process as those in (a) and (b), respectively, except for the strain direction (+45°). (e) The complex stripe pattern formed after subsequent annealing and cooling without external strain.

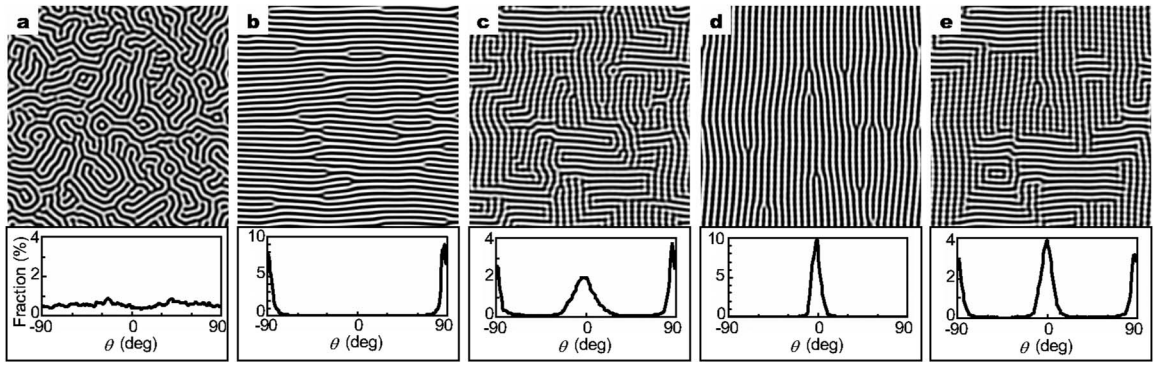

FIG. 3. Sequential pattern changes in model simulations. The upper panels show z of a cell (25.6×25.6 μm^2). The lower panels show the corresponding stripe orientation histograms. (a) The complex stripe pattern evolved (10^4 steps) without external strain. (b) The aligned stripe pattern z_a evolved under compressive strain in y (0°) without the memory effect. (c) The quasibiaxial stripe pattern formed after strain unloading with $z_m=0.1z_a$. (d) Subsequently formed aligned pattern under compression with $z_m=0.1z_a$. (e) Subsequently formed quasibiaxial stripe pattern after unloading with $z_m=0.1z_a$. States in (a)–(e) qualitatively correspond to those in Figs. 1(a), 1(d), 1(e), 2(a), and 2(b), respectively. The state in (a) also corresponds to that in Fig. 2(e), because the identical random initial configuration, which is related to the inherent imperfections, triggers an identical pattern.

identical to the pattern obtained first [Fig. 1(a)]. The pattern becomes stable again against mechanical perturbations at room temperature indicating the reacquisition of the pattern memory; the large basin of attraction of the original pattern reappears on the associated potential. This result possibly suggests that inherent imperfections in the effective hardness, which is related to roughness or density distribution, trigger the identical complex pattern only when the pattern forms without external strain.

A model based on the mechanics of a slightly deflected plate and the memory effect for a specific pattern [25] is used to describe this system qualitatively. The system is expressed by a plate with thickness h, elastic modulus E_1, and Poisson's ratio ν_1, which is supported by a soft elastic substrate with elastic modulus E_2 and Poisson's ratio ν_2, where we approximately set $(h, E_1/E_2, \nu_1, \nu_2)=(19\ \text{nm}, 10^4, 0.2, 0.48)$ [1–4]. The net potential energy with respect to the surface profile $z(x,y)$ reads $U(z)=U_b(z)+U_i(z)+U_s(z)$, where U_b, U_i, and U_s are potentials for the plate bending, the in-plane plate deformation, and the soft substrate deformation, respectively.

The plate bending potential reads $U_b=\int\int D[2H^2-(1-\nu_1)K]dxdy$, where D is the flexural rigidity of the plate, i.e., $D=E_1h^3/[12(1-\nu_1^2)]$, and H and K are the mean and Gaussian curvatures, respectively [5]. The in-plane plate deformation potential is approximated using the expression for isotropic plane deformation, which is the sum of the simple and shear strain energies, i.e., $U_i=[\varepsilon_x^2+2\nu_1\varepsilon_x\varepsilon_y+\varepsilon_y^2]E_1hA/[2(1-\nu_1^2)]+\gamma^2E_1hA/[4(1+\nu_1)]$, where A is the surface area of interest, and ε_x, ε_y, and γ are the effective mean strains. The strains are $\varepsilon_x=\{[\int\int(1+\partial_x^2)^{1/2}dxdy]/\int dy-\alpha_xL_{x0}\}/\alpha_xL_{x0}$, $\varepsilon_y=\{[\int\int(1+\partial_y^2)^{1/2}dxdy]/\int dx-\alpha_yL_{y0}\}/\alpha_yL_{y0}$, and $\gamma=[(\int\int\partial_x\partial_ydxdy)-\gamma_0]/A$, where ∂_β is the differential of z with respect to $\beta(=x$ or $y)$, α_β is the ratio of the neutral lateral length of the plate to that of the soft substrate in the β direction, and $L_{\beta0}$ is the lateral neutral length for the soft substrate in the β direction. The isotropic thermal expansion of the PDMS substrate during the hard film formation is assumed for the complex stripe pattern, $\alpha_x=\alpha_y=\alpha=1.015$ and $\gamma_0=0$. The soft substrate potential is defined as $U_s=\int\int[E_2(z-z_m)^2/\{4(1-\nu_2^2)\}+13E_2(z-z_m)^4]dxdy$, where z_m is the memorized configuration. The first term expresses the simple deformation in the z direction [5,6]. The second term approximates roughly the effect of the shear deformation. The memory effect is introduced as the space-dependent shift $z_m(x,y)$ of the neutral point for U_s, which is physically attributable to the irreversible material flow in the soft substrate during wrinkling, as the first approximation for simplicity.

The surface profile z evolves according to $\eta\,\partial z(x,y,t)/\partial t=-\partial U[z(x,y,t)]/\partial z(x,y,t)$, where η is the damping coefficient. Actual simulations are conducted by discretizing the equation in space and time with appropriate intervals. The surface profile z is represented by the 256^2 grid of a square lattice under a periodic boundary condition. For the strain perturbation in the x or y directions, the grid intervals are gradually changed in the directions parallel and vertical to the strain directions by factors of $(1+\kappa)$ and $(1-\nu_2\kappa)$, respectively, where κ is external strain and is changed from 0 to -0.008.

Figure 3(a) shows an evolved stripe pattern z_i with $z_m(x,y)\equiv0$. The initial random configuration was taken. One might see the similarity in Fig. 3(a) and Fig. 1(a). Aligned stripes are obtained when the pattern is evolved under external strain ($\kappa=-0.008$) in the y direction [Fig. 3(b)], corresponding to Fig. 1(d). Assuming that the aligned pattern z_a is memorized at this step, we set $z_m(x,y)=sz_a(x,y)$ with $s=0.1$. The constant s is the parameter of the memory strength and related to the degree of the irreversible material viscous flow in the soft substrate (in the vicinity of the surface) during wrinkling on cooling. Qualitatively speaking, the lower value for s indicates the higher viscosity of the soft substrate during the pattern formation. Note that the viscosity is assumed to be infinite at room temperature. Therefore, the value of s is constant. The value (0.1) for s is chosen. With the value, the complex pattern z_i with $z_m=sz_i$ is retrieved even after the strain perturbation [25], as has been observed experimentally [19]. Then, the strain is unloaded, resulting in

the quasibiaxial pattern z_b [Fig. 3(c)], which qualitatively corresponds to Figs. 1(c) and 1(e). The pattern z_b is aligned by compression in the x direction [Fig. 3(d)]. The strain-unloaded pattern appears as a different quasibiaxial pattern [Fig. 3(e)] compared to z_b. The statistical properties (histograms) of the stripe orientation are also in good agreement with the corresponding experimental results concerning the relative peak height and sharpness.

Although the model omits various physical details, the simulation shows that the quasibiaxial pattern evolves from the aligned stripes by strain. The quasibiaxial patterns can irreversibly change depending on the subsequent mechanical perturbation. The newly created memory of the aligned stripes becomes ineffective in terms of the retrieval of the pattern without a specific external strain in the memorized direction. Therefore, in the state without external strain, many local metastable states on the associated potential are created, which correspond to the various (quasibiaxial) patterns with different statistical natures of stripe orientation.

In conclusion, we demonstrate that the pattern in the state without external strain can be modulated by the ACU process and, therefore, the memory of the pattern is mainly created during pattern formation. The patterns produced through the ACU process are unstable against the mechanical perturbation at room temperature, because many local metastable states are created on the associated potential surface in place of a global minimum with the large basin of attraction. The ACU process is repeatable. Further investigations of the effect of the viscoelastic property of the material and time for the pattern formation will be required for detailed understanding of the system. However, the abilities to control the statistical nature of stripe orientation and the pattern stability suggest the possibility of fabricating nanomicroscale mechanical elements, which function cooperatively based on spontaneous organization in response to external global or local perturbations (inputs), e.g., mechanical [19,27], thermal, chemical perturbations, and so on.

We acknowledge informative discussions with C. Kamaga, R. Aihara, and H. Suetani.

[1] N. Bowden *et al.*, Nature (London) **393**, 146 (1998).
[2] N. Bowden *et al.*, Appl. Phys. Lett. **75**, 2557 (1999).
[3] D. B. H. Chua, H. T. Ng, and S. F. Y. Li, Appl. Phys. Lett. **76**, 721 (2000).
[4] W. T. S. Huck *et al.*, Langmuir **16**, 3497 (2000).
[5] S. Timoshenko and S. Woinowsky-Krieger, *Theory of Plate and Shells* (McGraw-Hill, New York, 1959).
[6] H. G. Allen, *Analysis and Design of Structural Sandwich Panels* (Pergamon, New York, 1969).
[7] E. Cerda and L. Mahadevan, Phys. Rev. Lett. **90**, 074302 (2003).
[8] L. Golubovic, D. Moldovan, and A. Peredera, Phys. Rev. Lett. **81**, 3387 (1998).
[9] T. Tanaka *et al.*, Nature (London) **325**, 796 (1987).
[10] M. C. Cross and P. C. Hohenberg, Rev. Mod. Phys. **65**, 851 (1993).
[11] M. Seul and D. Andelman, Science **267**, 476 (1995).
[12] C. Bowman and A. C. Newell, Rev. Mod. Phys. **70**, 289 (1998).
[13] P. Ball, *The Self-Made Tapestry* (Oxford University Press, New York, 2001).
[14] M. I. Rabinovich, A. B. Ezersky, and P. D. Weidman, *The Dynamics of Patterns* (World Scientific, Singapore, 2000).
[15] H. Möhwald, Thin Solid Films **159**, 1 (1988).
[16] M. Seul and R. Wolfe, Phys. Rev. Lett. **68**, 2460 (1992).
[17] C. Harrison *et al.*, Science **290**, 1558 (2000).
[18] M. Shimomura and T. Sawadaishi, Curr. Opin. Colloid Interface Sci. **6**, 11 (2001).
[19] T. Ohzono and M. Shimomura, Phys. Rev. B **69**, 132202 (2004).
[20] D. Moldovan and L. Golubovic, Phys. Rev. Lett. **82**, 2884 (1999).
[21] N. Sridhar, D. J. Srolovitz, and Z. Suo, Appl. Phys. Lett. **78**, 2482 (2001).
[22] R. Huang and Z. Suo, J. Appl. Phys. **91**, 1135 (2002).
[23] P. J. Yoo and H. H. Lee, Phys. Rev. Lett. **91**, 154502 (2003); P. J. Yoo, K. Y. Suh, H. Kang, and H. H. Lee, *ibid.* **93**, 034301 (2004).
[24] N. Uchida, Physica D **205**, 267 (2005).
[25] T. Ohzono and M. Shimomura, Jpn. J. Appl. Phys., Part 1 **44**, 1055 (2005).
[26] D. A. Egolf, I. V. Melnikov, and E. Bodenschatz, Phys. Rev. Lett. **80**, 3228 (1998).
[27] T. Ohzono and M. Shimomura, Langmuir **21**, 7230 (2005).